Retinoic acid receptor-related orphan receptor α stimulates adipose tissue inflammation by modulating endoplasmic reticulum stress

Received for publication, February 20, 2017, and in revised form, July 6, 2017 Published, Papers in Press, July 11, 2017, DOI 10.1074/jbc.M117.782391

Yin Liu[1], **Yulong Chen**[1], **Jinlong Zhang**[1], **Yulan Liu, Yanjie Zhang, and Zhiguang Su**[2]
From the Molecular Medicine Research Center, West China Hospital, State Key Laboratory of Biotherapy, Sichuan University, Chengdu 610041, Sichuan, China

Edited by Dennis R. Voelker

Adipose tissue inflammation has been linked to metabolic diseases such as obesity and type 2 diabetes. However, the molecules that mediate inflammation in adipose tissue have not been addressed. Although retinoic acid receptor-related orphan receptor α (RORα) is known to be involved in the regulation of inflammatory response in some tissues, its role is largely unknown in adipose tissue. Conversely, it is known that endoplasmic reticulum (ER) stress and unfolding protein response (UPR) signaling affect the inflammatory response in obese adipose tissue, but whether RORα regulates these processes remains unknown. In this study, we investigate the link between RORα and adipose tissue inflammation. We showed that the inflammatory response in macrophages or 3T3-L1 adipocytes stimulated by lipopolysaccharide, as well as adipose tissue in obese mice, markedly increased the expression of RORα. Adenovirus-mediated overexpression of RORα or treatment with the RORα-specific agonist SR1078 enhanced the expression of inflammatory cytokines and increased the number of infiltrated macrophages into adipose tissue. Furthermore, SR1078 up-regulated the mRNA expression of ER stress response genes and enhanced phosphorylations of two of the three mediators of major UPR signaling pathways, PERK and IRE1α. Finally, we found that alleviation of ER stress using a chemical chaperone followed by the suppression of RORα induced inflammation in adipose tissue. Our data suggest that RORα-induced ER stress response potentially contributes to the adipose tissue inflammation that can be mitigated by treatment with chemical chaperones. The relationships established here between RORα expression, inflammation, and UPR signaling may have implications for therapeutic targeting of obesity-related metabolic diseases.

The prevalence of obesity, likely caused by a global shift toward consumption of energy-dense foods and a sedentary lifestyle, is now considered to be a major public health epidemic in both developed and developing countries. Obesity, which is defined as abnormal or excessive fat accumulation in adipose tissues, is associated with chronic low-grade inflammation (1). Obese adipose tissue is characterized by enhanced infiltration of macrophage and various T-lymphocytes, as well as the release of abundant pro-inflammatory cytokines, *e.g.* IL-6 and TNF-α (2, 3). The inflammatory processes in adipose tissue contribute to several obesity-associated health problems, including insulin resistance, type 2 diabetes, cardiovascular disease, fatty liver, airway disease, musculoskeletal disorders, and a variety of cancers (4). Although the features of chronic inflammation in obese adipose tissue are clearly defined, the molecules that mediate inflammation in adipose tissue are not well understood.

Retinoic acid receptor-related orphan receptor α (RORα)[3] is a ubiquitously expressed nuclear hormone receptor (5). Numerous studies have demonstrated that RORα modulates various cell functions and implications in the regulation of inflammatory response (6, 7). However, its effects on the inflammatory response are inconsistent. *In vitro* stimulation of peritoneal macrophages from staggerer (RORα sg/sg) mice, a natural mutant strain deficient in RORα expression because of a deletion in the RORα gene (8), by LPS results in an elevated expression of IL-1α, IL-1β, and TNF-α (9). Overexpression of RORα in human primary smooth muscle cells inhibits TNF-α-induced expression of IL-6, IL-8, and cyclooxygenase-2 (10). In contrast, other studies have demonstrated that RORα functions as a critical pro-inflammatory factor. The RORα sg/sg mice deficient in RORα exhibit an attenuated allergic lung inflammatory response (11). In addition, the infiltration of macrophages and the expression of many inflammatory genes are greatly reduced in adipose tissue of RORα sg/sg mice fed with a high-fat diet (12). These observations suggest that the effect of RORα on inflammatory response appears to be cell- and tissue-dependent. The potential effects of RORα on inflammation response in adipocyte and adipose tissue are largely unknown.

Endoplasmic reticulum (ER) is primarily recognized as the site of synthesis and trafficking of secreted and integral membrane proteins. Perturbations in ER homeostasis can create a condition defined as ER stress. Cells respond to ER stress

This work was supported by National Natural Science Foundation of China Grant 31071108 and Sichuan Province Science and Technology Support Program Grant 2015SZ0140. The authors declare that they have no conflicts of interest with the contents of this article.
[1] These authors contributed equally to this work.
[2] To whom correspondence should be addressed. Tel.: 86-28-85164103; Fax: 86-28-85164092; E-mail: zhiguang.su@scu.edu.cn.

[3] The abbreviations used are: RORα, retinoic acid receptor-related orphan receptor α; Ad-RORα, recombinated adenovirus encoding RORα; ER, endoplasmic reticulum; UPR, unfolding protein response; SVF, stromal-vascular fraction; eIF, eukaryotic translational initiating factor; GTT, glucose tolerance test; ITT, insulin tolerance test; 4-PBA, 4-phenyle-butyric acid; qRT-PCR, quantitative RT-PCR.

© 2017 by The American Society for Biochemistry and Molecular Biology, Inc. Published in the U.S.A.

through three major signaling pathways mediated by PERK (PKR-like ER kinase), IRE1 (inositol-requiring enzyme 1), and ATF6 (activating transcription factor 6). The activity of these three proteins collectively leads to an ER-specific unfolded protein response (UPR) (13, 14). Recently, ob/ob genetic and diet-induced obese mice were reported to reveal up-regulation of ER stress markers in adipose tissue (15, 16). ER stress and UPR signaling have been shown to affect inflammation in obese adipose tissue (16–19). Whether RORα regulates ER stress and UPR in adipose tissue and the mechanisms responsible for ER stress-mediated inflammation of adipose tissue have not been addressed.

The aim of this study was to examine the roles of RORα in adipose tissue inflammation and ER stress response. Our results demonstrated that RORα is potently induced by inflammatory stimuli in macrophages, and RORα positively regulated the inflammatory response in obese adipose tissue. Furthermore, we provided evidence indicating that RORα-induced inflammation is related to an effect on ER stress response in adipose tissue. Our study further supports evidence that RORα enhanced the UPR signaling pathway. Alleviation of ER stress response using the chemical chaperone 4-phenyle-butyric acid could suppress the RORα-induced inflammatory response in obese adipose tissue.

Results

Inflammation stimulates RORα expression

To determine the regulation of RORα in responses to inflammatory mediator, we investigated the effect of LPS on expression of RORα in mouse primary peritoneal macrophages and RAW264.7 cells. LPS markedly increased the production of TNF-α and IL-6 in thioglycolate-elicited peritoneal macrophages or RAW264.7 cells (Fig. 1*a*). A time course of LPS treatment of murine macrophages or RAW264.7 cells revealed that mRNA expression of RORα was potently induced at early time points, with mRNA levels peaking at 2 h post-treatment (Fig. 1*b*). Western blot analysis showed that RORα protein significantly increased at 2 h and remained elevated until 4 h after stimulation (Fig. 1*c*). RORα protein expression was further studied using immunofluorescence microscopy. Strong cytoplasm staining was observed as early as 2 h after stimulation, with RORα protein accumulated in the nucleus at 4 h post-treatment (Fig. 1*d*).

Obese adipose tissue is characterized by chronic inflammation involving inflammatory cell infiltration and activation of the cytokine network (1, 2). Ob/ob mice develop insulin resistance and inflammation in various tissues and represent a well established model of obesity and type 2 diabetes. To obtain further evidence that inflammation modulates the expression of RORα, we determined RORα expression in ob/ob mice. In agreement with published reports, the mRNA expression levels of selected inflammatory cytokines (TNF-α, IL-6, and MCP1), as well as the macrophage-specific marker F4/80, were significantly increased in genetic obese (ob/ob) mice (Fig. 1*e*). Additionally, we observed that the protein levels of RORα were significantly up-regulated in the mature adipocytes of epididymal adipose tissue from obese mice, but not in the stromal-vascular fraction (SVF), which is a source of preadipocytes and macrophages (Fig. 1*f*). These observations provided a potential link between the elevated inflammatory mediators and RORα in obese adipose tissue.

RORα induces inflammatory response in adipose tissue

To evaluate the effect of RORα on the inflammatory response, we first measured the productions of inflammatory cytokines in 3T3-L1 adipocytes that were treated with SR1078, a synthetic ROR-specific agonist (20). We found that mRNA expression of the inflammatory genes TNF-α, IL-6, and MCP1 was significantly elevated by SR1078 treatment (Fig. 2*a*). Treatment of SR1078 increased the protein level of RORα as previously observed (21). Transduction of recombinated adenovirus encoding RORα (Ad-RORα) also induced the expression of TNF-α, IL-6, and MCP1 (Fig. 2*b*).

We next examined the effect of RORα in the pro-inflammation *in vivo* using ob/ob mice and C57BL/6J mice treated with SR1078 or DMSO. The plasma concentrations of pro-inflammatory cytokines including TNF-α and IL-6 were significantly increased in SR1078-treated mice relative to controls (Fig. 2, *c* and *d*). Real-time quantitative PCR analysis of the expression of IL-6, TNF-α, and MCP1 mRNA in adipose tissue (Fig. 2, *e* and *f*) showed, as expected, that the transcripts of these molecules were significantly increased in SR1078-treated mice compared with DMSO-treated mice. Production of cytokines during an inflammatory response is generally accompanied by recruitment of cells of the immune system to the site of injury or infection. Indeed, the gene expression levels of the mouse macrophage-specific marker F4/80 were also significantly elevated (Fig. 2, *e* and *f*). Also consistent with an increase in F4/80 transcript, immunochemistry staining showed that the infiltration of F4/80-positive macrophage into the adipose tissue was significantly increased in SR1078-treated mice compared with DMSO-treated mice (Fig. 2*g*). Flow cytometric analysis of SVF isolated from adipose tissue indicated that the percentage of SVF-associated macrophages ($F4/80^+/Cd11b^+$) was greatly increased in SR1078-treated mice (Fig. 2*h*). These findings provide evidence of RORα stimulating inflammatory response in adipose tissue.

RORα stimulates ER stress and UPR signaling

UPR signaling, in addition to its canonical role in alleviating ER stress, has recently been shown to be involved in inflammation in adipose tissue (16, 17). We first examined the effects of ER stress on the RORα expression in cultured adipocytes. 3T3-L1 adipocytes were stimulated with 3 μg/ml of tunicamycin, which causes ER stress by inhibiting *N*-linked glycosylation (22). In addition to the ER stress markers, such as BIP (binding protein) and CHOP (c/EBP-homologous protein), tunicamycin treatment significantly up-regulated both mRNA expression (Fig. 3*a*) and protein level (Fig. 3*b*) of RORα in a time-dependent manner. Next we examined ER stress in the obese adipose tissue. Compared with matched lean controls, the expression levels of ER stress markers such as BIP, phosphorylated PERK, phosphorylated eukaryotic translational initiating factor 2α (eIF2α), and ATF4 (activating transcription factor 4) were significantly elevated in adipose tissue of obese mice (Fig. 3*c*).

ASBMB

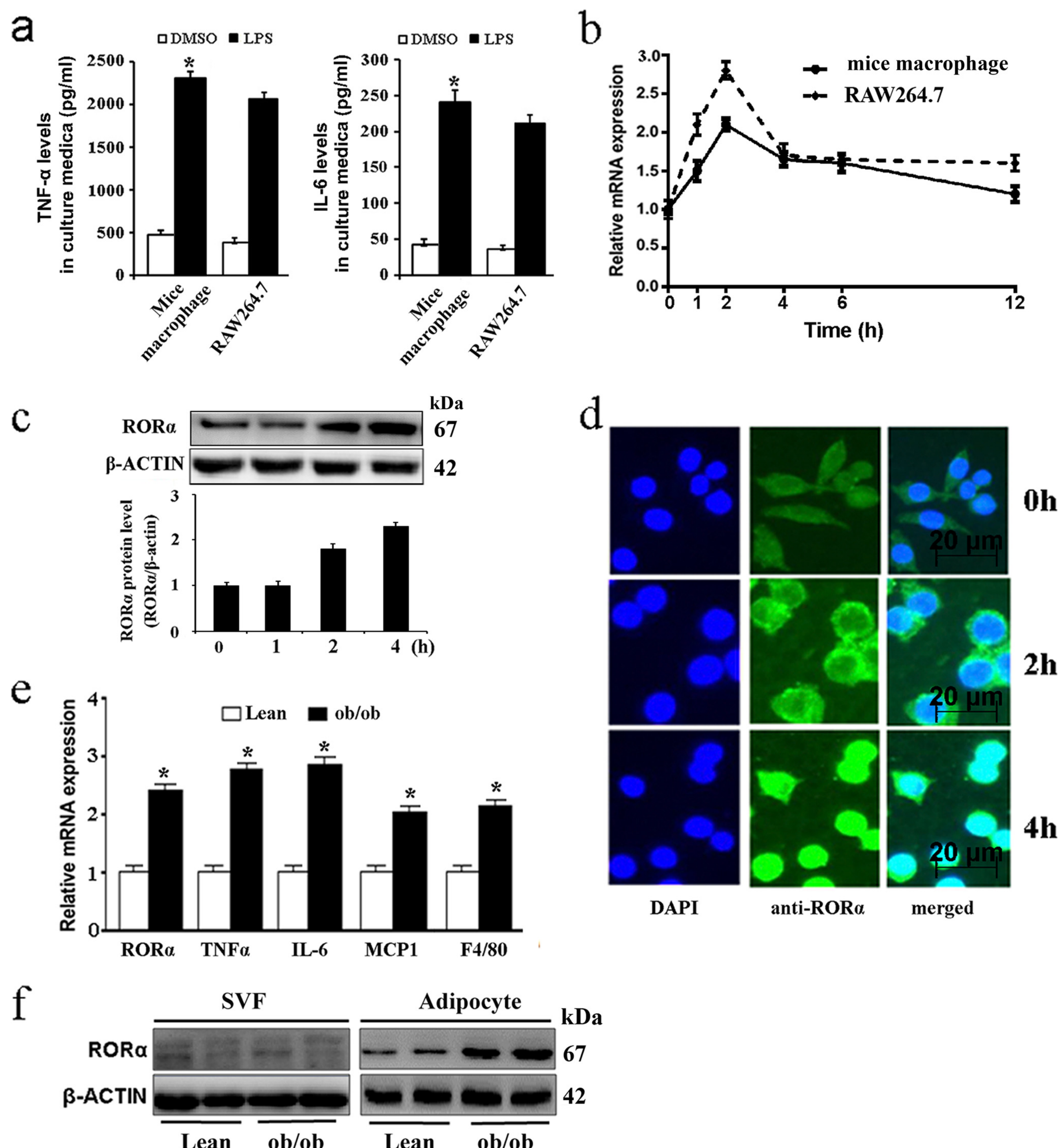

Figure 1. Expression of RORα is induced by inflammatory stimuli. *a–d*, murine primary macrophages and RAW264.7 cells (5×10^5 cells/well) were stimulated with DMSO or 100 ng/ml LPS. *a*, levels of TNF-α (*left panel*) and IL-6 (*right panel*) in culture medium of primary macrophages and RAW264.7 cells were determined by ELISA. *b*, RORα mRNA expression in the indicated times was analyzed by qRT-PCR. *c*, RORα protein levels were determined by Western blotting in primary macrophages in the indicated times. *d*, RAW264.7 cells were treated with LPS (100 ng/ml) for the indicated times. The cells were then permeated and stained with antibody to RORα and counterstained with DAPI. *e*, mRNA expression levels of inflammatory cytokines in adipose tissues derived from 8-week-old obese (ob/ob) and lean (C57BL/6J) mice ($n = 5$ each group). *f*, RORα protein levels in adipocytes and SVF of white adipose tissue from obese and lean mice. The values are means ± S.D. of three independent experiments. *, $p < 0.05$ *versus* control (unpaired Student's *t* test).

Additionally, the RORα protein level was significantly up-regulated in obese mice (Fig. 3*c*). Taken together, these results suggested that ER stress induction enhances RORα expression in adipocytes.

To examine whether RORα potentially lead to induction of ER stress, we performed *in vitro* experiments in 3T3-L1 adipocytes that were treated with SR1078. Gene expression analysis demonstrated that elevation of RORα induced by SR1078 significantly increased the expression of ER stress markers, including Chop, Atf4, Edem (ER degradation enhancer mannosidase), Erdj4 (ER DnaJ homolog 4), and Pdi (protein disulfide isomerase) (Fig. 4*a*). Transduction of Ad-RORα also induced

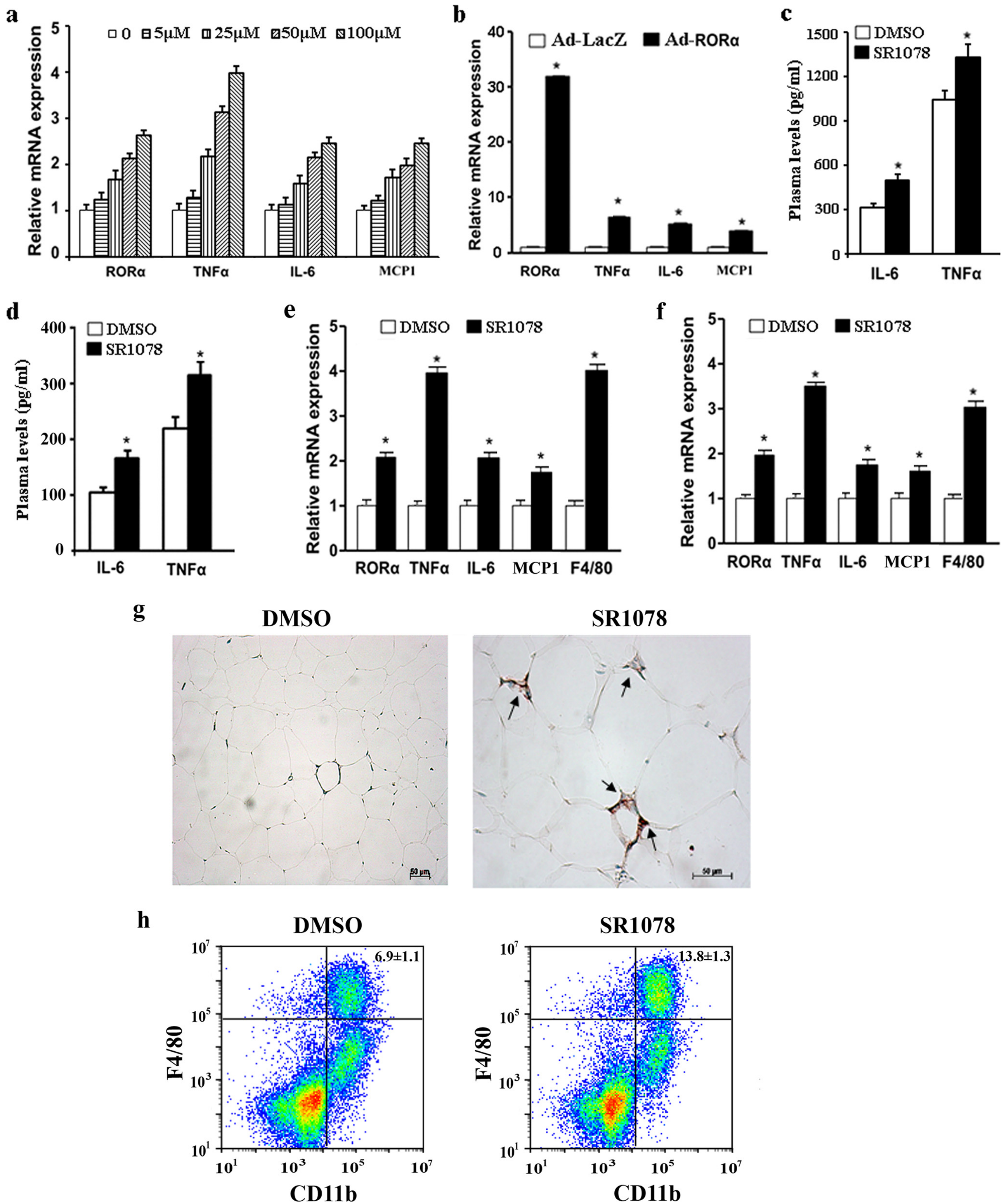

Figure 2. Effects of RORα on the inflammatory response. *a* and *b*, 3T3-L1 adipocytes were treated with indicated concentrations of SR1078 (*a*) or infected by Ad-LacZ or Ad-RORα for 24 h (*b*). mRNA expression levels of RORα and inflammatory cytokines were measured by qRT-PCR. *c–h*, 8-week-old mice were orally fed SR1078 (100 mg/kg body weight, twice daily) or DMSO for 10 days (5 mice/group). *c* and *d*, levels of IL-6 and TNF-α in the plasma from ob/ob mice (*c*) and C57BL/6J mice (*d*) were determined by ELISA. *e* and *f*, mRNA expression levels of RORα and inflammatory cytokines in white adipose tissues from ob/ob mice (*e*) and C57BL/6J mice (*f*) were measured by qRT-PCR. *g*, immunofluorescence staining of macrophage marker F4/80 in white adipose tissue. Treatment with SR1078 promoted macrophage infiltration into adipose tissue (*arrows*). *h*, flow cytometry analysis of macrophages in SVF cells from epididymal fat of mice treated with DMSO or SR1078. The percentage of the macrophage population (F4/80/CD11b cells) was significantly increased in SR1078-treated mice. The data represent means ± S.D. of three independent experiments. *, $p < 0.05$ *versus* vehicle treatment (DMSO) or Ad-LacZ infection.

ASBMB

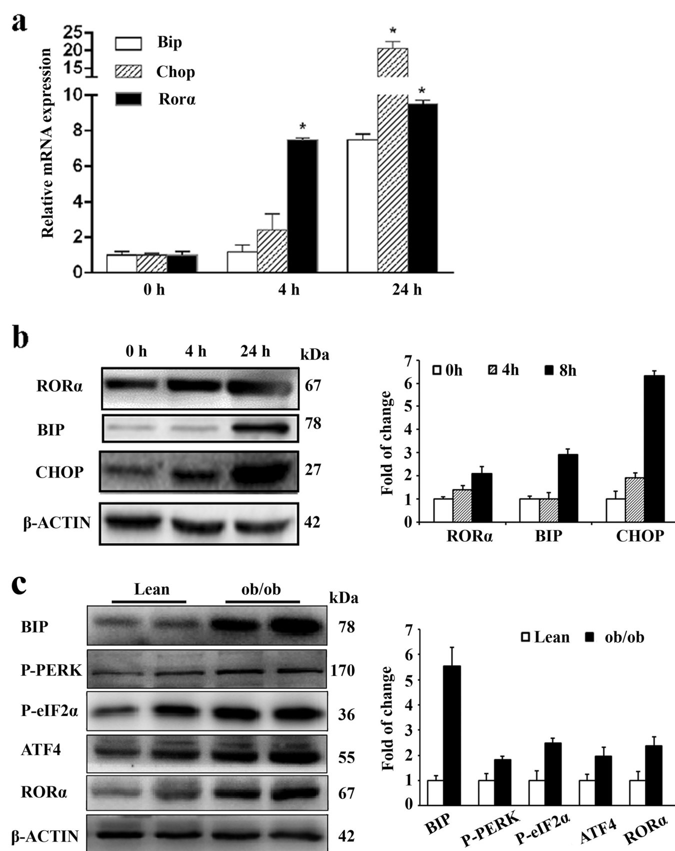

Figure 3. ER stress enhances RORα expression. *a* and *b*, 3T3-L1 adipocytes were stimulated with 3 μg/ml of tunicamycin for the indicated times. mRNA expression (*a*) and protein levels (*b*) of RORα and ER stress markers were measured by qRT-PCR and Western blotting, respectively. The values are means ± S.D. of three independent experiments performed in triplicate. *, $p < 0.05$ *versus* 0 h (unpaired Student's *t* test). *c*, ER stress indicators in adipose tissues of obese mice. Protein levels of BIP, PERK phosphorylation, eIF2α phosphorylation, and ATF4 were examined in adipose samples of ob/ob and lean (C57BL/6J) mice at the age of 8 weeks.

the expression of these ER stress markers (Fig. 4*b*). We then examined whether RORα induces a higher level of ER stress in adipose tissue derived from ob/ob mice treated with SR1078. As shown in Fig. 4*c*, the levels of BIP and CHOP proteins were significantly up-regulated in epididymal fat pads of SR1078-treated mice. We also determined the mRNA expression levels of Edem1, Erdj4, and Pdi; all of these ER stress markers were significantly elevated in SR1078-treated mice (Fig. 4*d*).

Subsequently, we focused on downstream events of RORα and UPR signaling. The three major UPR signaling pathways (mediated by PERK, IRE1, and ATF6) that are activated by ER stress are known to stimulate the expression of inflammatory cytokines in several cell types (23). Therefore, we examined the effects of RORα on the levels of proteins in all three UPR sub-pathways in ob/ob mice by administering them to SR1078. Compared with the DMSO-treated mice, the phosphorylations of PERK and IRE1 were significantly up-regulated in adipose tissue derived from SR1078-treated mice, whereas the cleaved-ATF6 level was not notably different between SR1078- and vehicle-treated mice (Fig. 4*e*). Activated PERK results in phosphorylation of eIF2α, which was demonstrated to modify level of ATF4 protein synthesis at the step of mRNA translation (24). Corresponding to the elevated PERK phosphorylation, phosphorylation of eIF2α and the ATF4 protein expression was significantly increased in SR1078-treated mice (Fig. 4*e*). IRE1 phosphorylation displays endoribonuclease activity, which cleaves its primary target, the mRNA encoding XBP1 (X-box-binding protein 1). As shown in Fig. 4*f*, SR1078 treatment significantly elevated the mRNA expression of splicing of Xbp1 (sXBP1) in a time-dependent manner. These results suggested that RORα induces ER stress and is followed by activation of the UPR signaling pathway in adipose tissue.

Suppression of RORα in ob/ob mouse reduces ER stress and improves glucose tolerance

To further confirm the effect of RORα on ER stress and UPR signaling, we treated ob/ob mice with SR1001, a synthetic inverse agonist of RORα (25). As shown in Fig. 5*a*, compared with the DMSO-treated mice, the levels of BIP and CHOP proteins were significantly down-regulated in the epididymal fat pads of SR1001-treated mice. In addition, SR1001 treatment significantly attenuated the protein expression of phosphorylations of IRE1 and eIF2α (Fig. 5*b*). These results confirmed the role of RORα in regulating ER stress and UPR signaling pathway in adipose tissue.

ER stress may compromise glucose metabolism and insulin sensitivity, key indicators of the development of type 2 diabetes. The reduced ER stress by SR1001 prompted us to determine whether suppression of RORα can improve glucose intolerance and insulin sensitivity in ob/ob mice. Glucose-tolerance tests (GTTs) and insulin-tolerance tests (ITTs) were performed. GTT experiments indicated that suppression of RORα by SR1001 improved glucose intolerance (Fig. 5*c*), ITT experiments also suggested that RORα suppression enhances insulin sensitivity in ob/ob mice (Fig. 5*d*).

Alleviation of ER stress suppresses RORα-induced inflammatory response in obese mice

Based on the inductions of both ER stress and inflammation response by RORα, we hypothesized that RORα-induced ER stress could contribute to chronic inflammation in adipose tissue. To test this hypothesis, obese (ob/ob) mice were first orally administered SR1078 (500 mg/kg body weight) for 10 days and then were fed chemical chaperone 4-phenyle-butyric acid (4-PBA) for 10 days. Treatment with 4-PBA significantly reduced the protein levels of ER stress markers BIP and CHOP, whereas there is no notable difference in RORα levels (Fig. 6*a*). The mRNA expression levels of other downstream ER stress markers, including Edem1, Erdj4, and Pdi, were also significantly down-regulated (Fig. 6*b*). We then determined the plasma concentrations of TNF-α and IL-6 and observed that they were significantly decreased in mice treated with both SR1078 and 4-PBA compared with the mice only treated with SR1078 (Fig. 6*c*). Results from the mRNA expression analysis indicated that the expression levels of TNF-α, IL-6, and MCP1 in adipose tissue were significantly decreased in 4-PBA-treated mice relative to controls (Fig. 6*d*). Immunochemistry staining showed that treatment with 4-PBA reduced the SR1078-induced F4/80-positive macrophage infiltration into adipose tissue (Fig. 6*e*). The decrease in F4/80$^+$ macrophages was supported by flow cytometric analysis of inflammatory cell

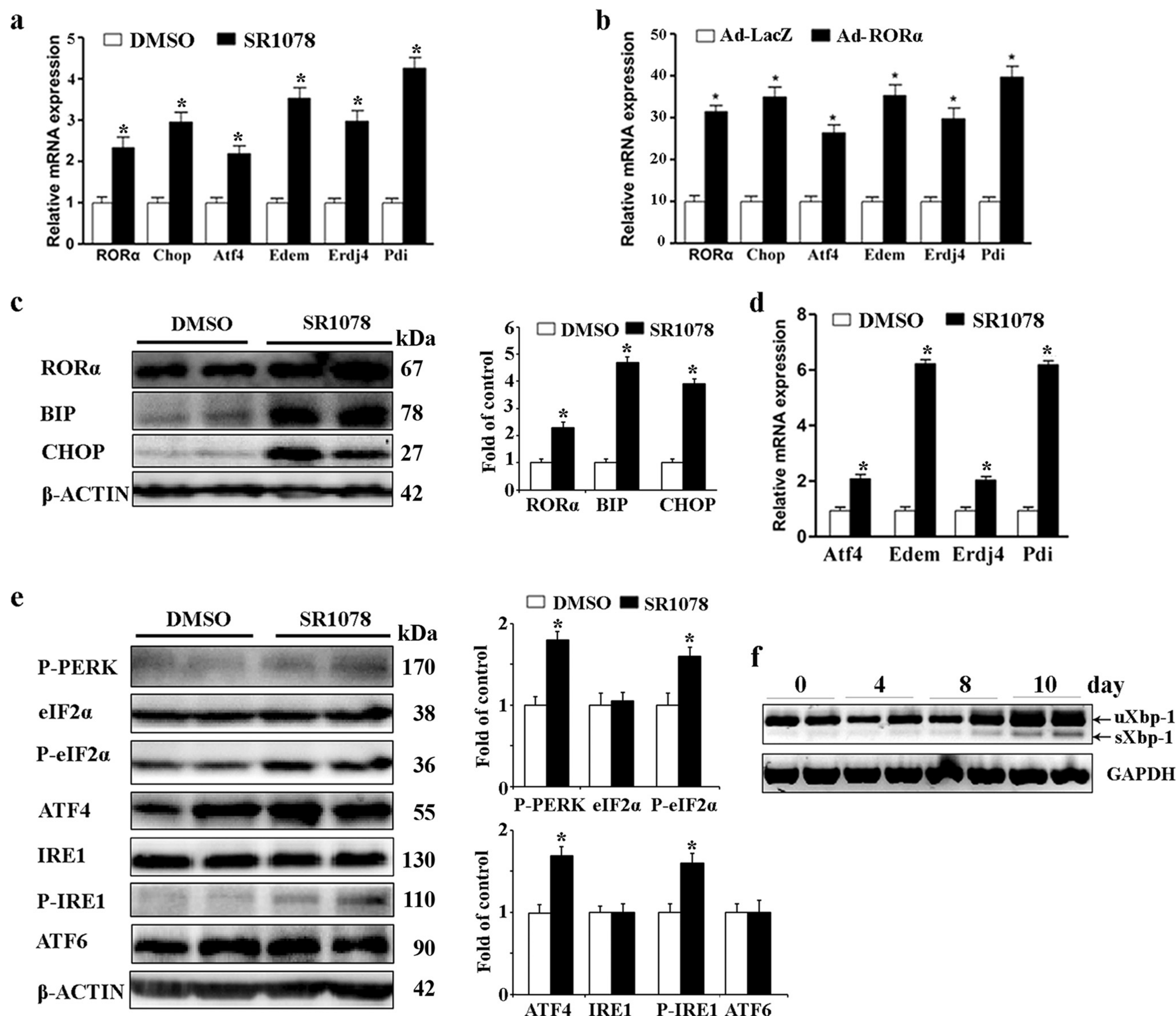

Figure 4. RORα stimulates UPR signaling. *a* and *b*, 3T3-L1 adipocytes were treated with 100 μM SR1078 (*a*) or infected by Ad-LacZ or Ad-RORα (*b*) for 24 h. mRNA expression of RORα and ER stress markers including Chop, Atf4, Edem, Erdj4, and Pdi was analyzed by qRT-PCR. *c–f*, SR1078 (100 mg/kg body, twice daily, $n = 5$) or DMSO ($n = 5$) was orally administered to 8-week-old ob/ob mice for 10 days. *c*, protein levels of BIP and CHOP were determined by Western blotting. *d*, mRNA expression of ER stress markers including Atf4, Edem1, Erdj4, and Pdi was measured by qRT-PCR. *e*, levels of proteins in the three major UPR signaling pathways (mediated by PERK, IRE1, and ATF6) were determined by Western blotting. *f*, XBP-1 expression in adipose tissue was examined by RT-PCR. ob/ob mice were treated with SR1078 for indicated times. Both the unspliced XBP-1 (uXbp-1) form of 246 bp and the spliced XBP-1(sXbp-1) form of 220 bp were amplified by RT-PCR in same reaction.

populations of SVF isolated from white adipose tissue. This analysis showed that the percentage of SVF-associated macrophages ($F4/80^+/Cd11b^+$) was greatly reduced in 4-PBA-treated mice (Fig. 6*f*). Taken together, these observations suggest that RORα-induced ER stress potentially regulate the elevated inflammatory response in adipose tissue.

Discussion

It is now well recognized that obesity is associated with chronic low-grade inflammation and that inflammatory processes play a key role in the development of obesity-associated pathologies. In this study, we showed that RORα stimulates inflammatory response in adipose tissue, which was alleviated by treatment with chemical chaperones that can suppress ER stress. Our results provide evidence indicating that RORα expression causes ER stress and activates UPR signaling in adipose tissue of ob/ob mice.

ER is an organelle with functions mostly in protein folding, maturation, transporting, and maintaining calcium homeostasis. When the ER becomes stressed because of the accumulation of unfolded/misfolded/mutated proteins, the UPR is triggered to restore ER homeostasis and normal function. The ER stress and UPR are initiated by three ER transmembrane protein sensors: PERK, IRE1, and ATF6 (18). In the present study, we demonstrated that the PERK subpathway was activated by RORα expression. It was reported that PERK signaling activates NF-κB (26), a transcriptional regulator that plays a central role in mediating the responses to inflammatory signaling. PERK mediates inhibition of protein translation via phosphorylation of eIF2a. Translation of IκBa, the main negative regulator of

ASBMB

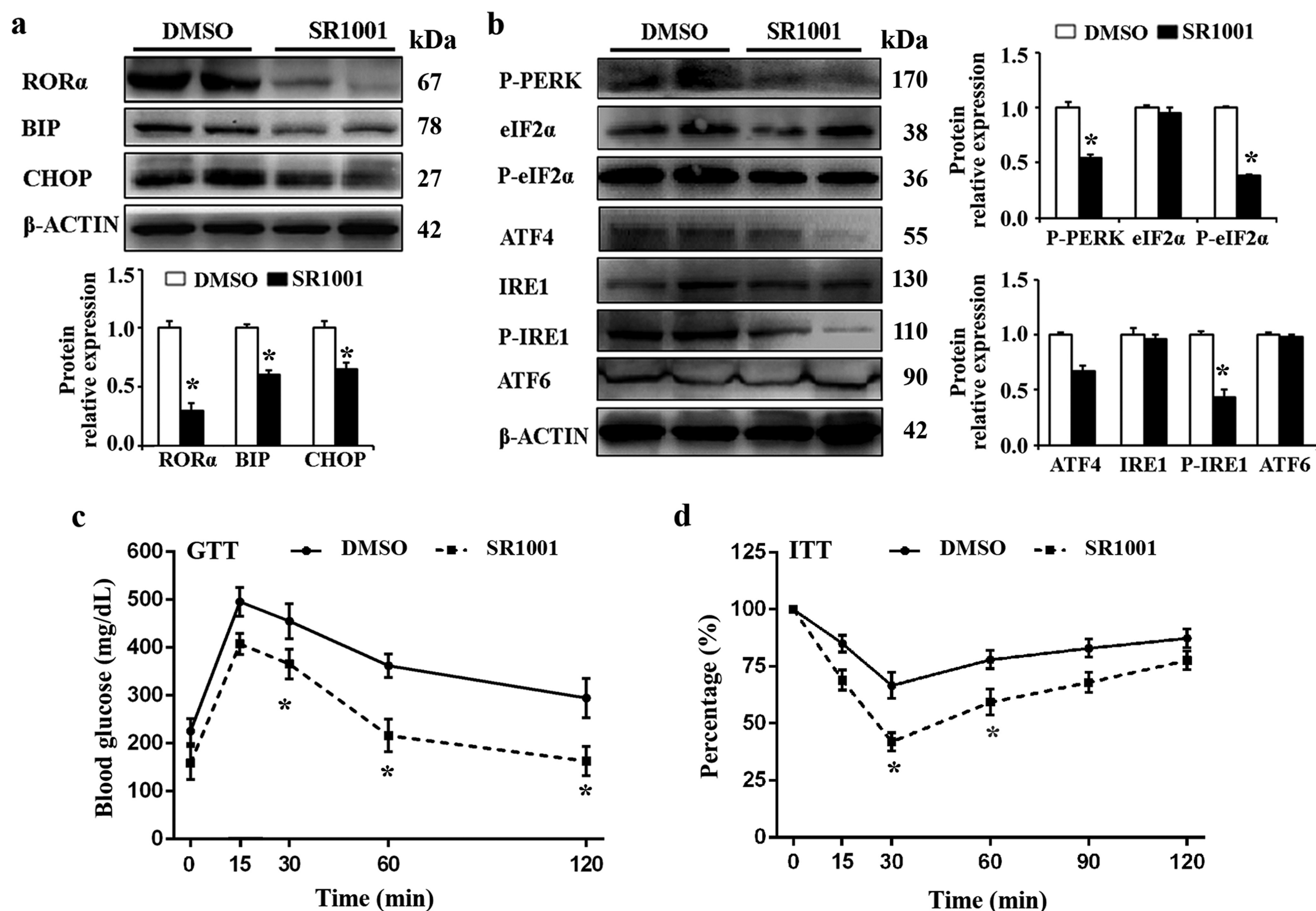

Figure 5. Suppression of RORα reduces ER stress and improves glucose tolerance. *a*, SR1001 (25 mg/kg body, twice daily, $n = 5$) or DMSO ($n = 5$) was orally administered to 8-week-old ob/ob mice for 10 days. Protein levels of BIP and CHOP were determined by Western blotting. *b*, levels of proteins in the three major UPR signaling pathways (mediated by PERK, IRE1, and ATF6) were determined by Western blotting. *c* and *d*, GTTs (*c*) and ITTs (*d*) were performed. The mice were injected with glucose (2 g/kg) or insulin (1 units/kg), and the blood glucose levels were measured at the indicated time points by a glucose meter. The values are presented as means ± S.D. *, $p < 0.05$ *versus* DMSO treatment.

NF-κB, is known to be inhibited by phosphorylation of eIF2a. A decrease in the translation of IκBa results in removal of inhibition of NF-κB activity and promotes the translocation of NF-κB from the cytoplasm to the nucleus. Therefore, the enhanced phosphorylations of PERK and its downstream eIF2α by RORα expression will attenuate IκBa inhibitory control and allow the induction of inflammatory genes. In addition to the PERK signaling pathway, IRE1 branch of the UPR is also activated by RORα expression. It was reported that the IRE1 signaling pathway directly activates JNK (27), an important inflammatory signaling mediator. JNK up-regulates the expression of inflammatory cytokines by activating the AP-1 (activator protein 1) transcription factor complex (28).

Understanding the mechanism by which RORα regulates inflammation could provide a potential therapeutic target for the treatment of obesity-related metabolic disorders. Because nuclear receptors function as ligand-dependent transcription factors, they provide excellent pharmacologic targets to interfere in (patho)physiologic processes; therefore, they may be very promising in yielding novel therapeutic strategies for human disease. Ligands for peroxisome proliferator-activated receptors, liver X receptors, and vitamin D3 receptors, which have been reported to significantly influence inflammatory responses (29), may be promising candidates for additional therapeutic strategies. The enhanced RORα-induced inflammatory response observed in the adipose tissue of ob/ob mice suggests a role for this nuclear receptor in the development of obesity-associated pathologies. Activation of the RORα receptor by endogenous ligands, such as cholesterol (30), might be implicated in the recently reported link between obesity and hypercholesterolemia. Synthetic, high-affinity antagonists could prevent these recently identified endogenous ligands from activating ROR, inhibit the activation of inflammatory genes, and have potential in the treatment of obesity and its associated disorders.

Our results revealed the possibility that attenuation of ER stress via inhibiting RORα may be an effective approach to reduce the risk of obesity and its complications. However, ER stress has various physiologic roles, including escape from apoptosis in cells with unfolded protein in the ER (27, 31), regulation of secretory cell differentiation or maturation (32), and maintenance of cellular homeostasis (33). Consequently, complete elimination of ER stress by agents that prevent ER stress could cause disadvantage for living cells and biological regulation. To develop the agents targeting RORα under clinical conditions, further studies are now needed to characterize the functional changes in cells dependent on ER stress.

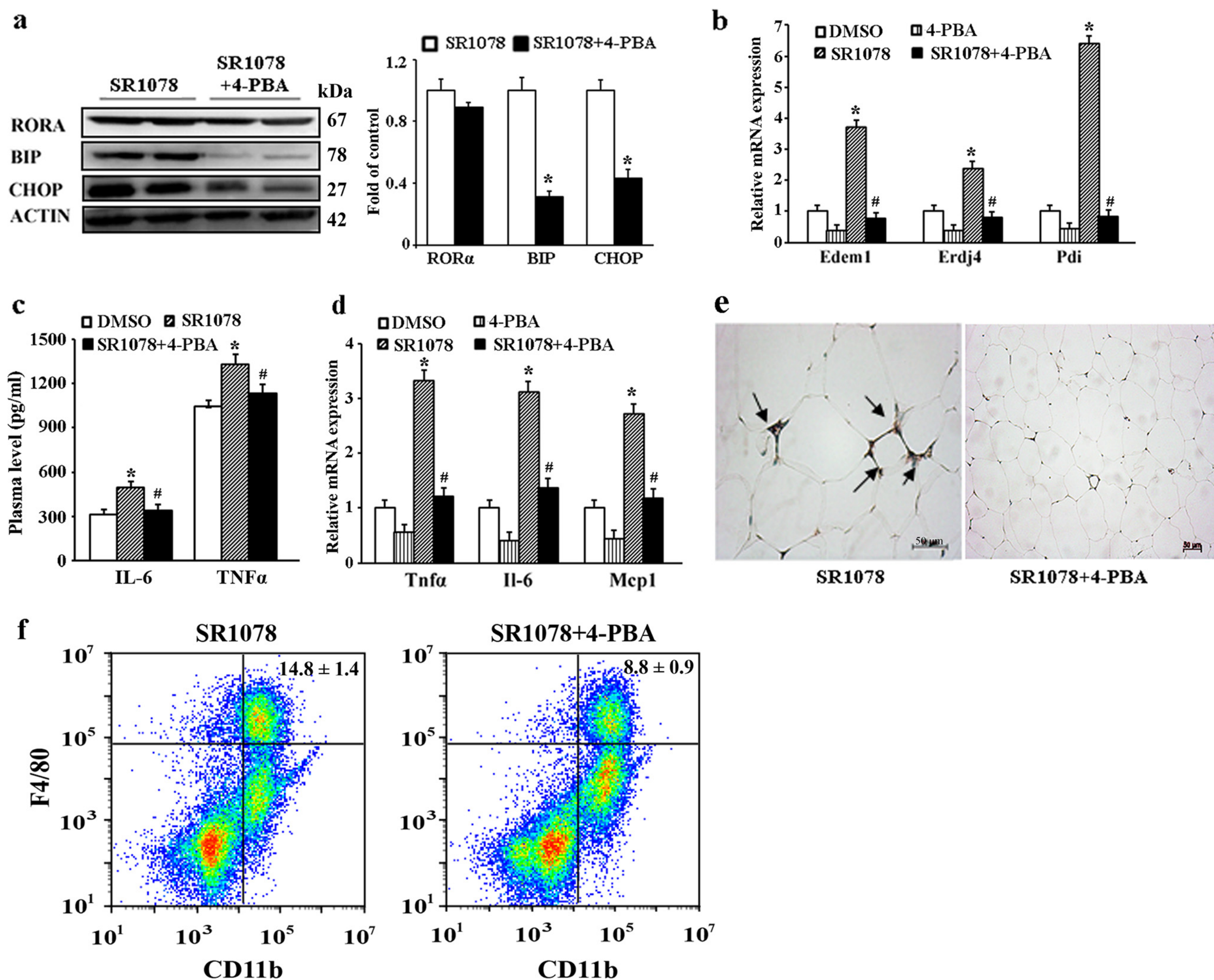

Figure 6. Effects of chemical chaperones 4-PBA on RORα-induced inflammatory response in obese mice. After 10 days of SR1078 treatment (100 mg/kg body, $n = 5$), ob/ob mice were orally administered 4-PBA at a dose of 1 g/kg/day for 10 days. *a*, protein levels of RORα and ER stress markers BIP and CHOP in adipose tissue were determined by Western blotting. *b*, mRNA expression of ER stress markers (EDEM, ATF4, and PDI) in adipose tissue was measured by qRT-PCR. *c*, levels of IL-6 and TNF-α in the plasma were determined by ELISA. *d*, mRNA expression of inflammatory cytokines (TNF-α, IL-6, and MCP1) in adipose tissue was measured by qRT-PCR. *e*, immunofluorescence staining of macrophage marker F4/80 in adipose tissue. The *arrows* indicate macrophage infiltration. Treatment with 4-PBA attenuated the SR1078-induced macrophage infiltration into adipose tissue. *f*, flow cytometry analysis of macrophages in SVF cells from epididymal fat pads of mice treated with both SR1078 and 4-PBA or SR1078 alone. The percentage of the macrophage population (F4/80/CD11b cells) was significantly reduced in mice treated with both SR1078 and 4-PBA compared with mice treated with only SR1078. The values are presented as the means ± S.D. *, $p < 0.05$ *versus* DMSO treatment; #, $p < 0.05$ *versus* SR1078 treatment (unpaired Student's *t* test).

Materials and methods

Reagents

LPS, DMSO, DMEM, penicillin, glutamine, streptomycin, SR1078, 3-isobutyl-methyl-xanthine, dexamethasone, insulin, Triton X-100, tunicamycin, 4-PBA, and secondary horseradish peroxidase-conjugated antibodies were obtained from Sigma-Aldrich. FBS was from Hyclone (Logan, UT). Lipofectamine 2000 and TRIzol reagent were from Invitrogen. ELISA kits for IL-6 and TNF-α were from Enzo Life Sciences (New York, NY). Antibodies against RORα (SC-22799), ATF6α (SC-22799), and β-actin (SC-47778) were from Santa Cruz Biotechnology (Santa Cruz, CA). Antibodies against BIP (no. 3177), CHOP (no. 2895), PERK (no. 3192), phospho-PERK (no. 3179), eIF2α (no. 5324), and IRE1 (no. 3294) were from Cell Signaling Technology (Danvers, MA). Antibodies against ATF4 (ET1603-37), phospho-eIF2α (ET1603-14), and F4/80 (RT1212) were from HuaAn Biotechnology (Hangzhou, China). Phospho-IRE1 (ab48187) antibody was from Abcam (Cambridge, UK). Antibodies against FITC-CD11b (no. 561688) and PE-F4/80 (no. 565410) were from BD Biosciences (Shanghai, China). SYBR Green Master Mix was from Applied Biosystems (Foster City, CA). All the chemicals were dissolved in the appropriate media solution or DMSO and then used at indicated concentration.

Cell culture, adipocyte differentiation, and treatment

RAW264.7 cells and mouse 3T3-L1 preadipocytes were obtained from American Type Culture Collection (Manassas, VA) and cultured in DMEM containing 4.5 g/liter glucose and 2 mM L-glutamine at 37 °C with a humidified 5% CO_2 atmosphere. The medium was supplemented with 10% (v/v) heat-inactivated FBS, 50 units/ml penicillin, and 50 mg/ml streptomycin. After reaching confluence, 3T3-L1 preadipocytes were

ASBMB

Table 1
Sequence of primers

Gene	Primer sequence (5′-3′) Forward	Reverse
Gapdh	GGTGAAGGTCGGTGTGAACG	CTCGCTCCTGGAAGATGGTG
RORα	CAGCAGAGCAATGCCACC	CGACCAAACTTGACAGCATC
TNFα (*Tnf*)	ATGGCCCAGACCCTCACACTCAGAT	GAAGAGAACCTGGGAGTAGACAA
IL-6	GACAACTTTGGCATTGTGG	ATGCAGGGATGATGTTCTG
Mcp1 (*Ccl2*)	CTTCTGTGCCTGCTGCTCATA	CTTTGGGACACTTGCTGCTG
F4/80 (*Adgre1*)	GTCAGATGATTCAGACGGAGTA	GGTCACAGTGCCACCAACAA
Bip (*Hspa5*)	GCCGAGACAACACTGACCTG	ACCACCGTGCCCACATCC
Chop (*Ddit3*)	TCCCTGCCTTTCACCTTGG	GGCTTTGGGATGTGCGTGT
Edem1	CGCGGAGACCCTTCCAATCT	CTTCCCAGAACCCTTATCGTAG
Erdj4 (*DNAJB9*)	GCCATGAAGTACCACCCTGACA	TCGTCTATTAGCATCTGAGAGTGT
Atf4	AAGTGAAGACTGAGAAATTGGATA	GCCTTACGGACCTCTTCTATC
Pdi (*Padi2*)	AATAGTCCCATTAGCAAAGGTG	ACCCACCACTGAGGCATCTT
Xbp-1	CCTTGTAGTTGAGAACCAGG	GGGGCTTGGTATATATGTGG

stimulated with differentiation medium consisting of growth medium supplemented with 0.25 mM 3-isobutyl-methyl-xanthine, 1 mM dexamethasone, and 1 mg/ml insulin. Two days after stimulation, the cells were placed in poststimulation medium containing DMEM, 10% FBS, and 1 mg/ml insulin. Fully differentiated adipocytes were used at 12–14 days after induction of differentiation. Mouse peritoneal macrophages were isolated from C57BL/6J mice after stimulation with an intraperitoneal injection of 2% thioglycolate solution (3 ml/mouse) as described (34). The cells were treated with LPS (100 ng/ml, 0–12 h) in the presence or absence of SR1078 (0–100 μM, 0–24 h).

Transfections

Ad-RORα was constructed as described (21) and then transfected into Hek293 cells by Lipofectamine 2000 to allow packaging and amplification of the Ad-RORα. The adenovirus was purified using Adeno-x™ virus mini purification kit, and the infective titer was determined by a limiting dilution plaque assay. The efficiency of adenoviral infection was examined by using the adenovirus Ad-RORα tagged with green fluorescent protein. Fully differentiated 3T3-L1 adipocytes were infected with adenovirus at the multiplicity of infection of 40 and cultured in 2% FBS medium for 4 h and then switched to regular growth medium. 48 h later, the cells were harvested for quantitative PCR or Western blotting.

Animals and treatments

Male C57BL/6J-Lep^{ob} leptin-deficient mice (ob/ob mice) and C57BL/6J (The Jackson Laboratory) were housed under a 12-h light/12-h dark cycle and followed free access to regular diet. At the age of 8 weeks, the mice were orally administered vehicle (DMSO, $n = 5$), SR1078 (100 mg/kg body weight/dose, two doses daily, $n = 5$), or SR1001 (25 mg/kg body weight, twice daily, $n = 5$) for 10 days. In 4-PBA assay, after the last SR1078 administration, the mice were fed 4-PBA (500 mg/kg body weight/dose, two doses daily) for 10 days with oral gavage, and the mice in the control groups received the same volume of DMSO. The mice were anesthetized with diethyl ether, and whole blood was collected by cardiac puncture. Plasma was obtained from whole blood by centrifugation and stored at −20 °C until assayed. Epididymal fat pads were removed and frozen immediately in liquid nitrogen until assayed. All experiments were in compliance with the National Institute of Health guide for care and use of laboratory animals and the international association for the study of pain research guidelines. Animal care and experimental procedures were approved by the ethics committee of animal experimentation of Sichuan University.

ELISA analysis

Plasma concentrations of IL-6 and TNF-α were determined by ELISA according to the manufacturer's instructions.

Glucose and insulin tolerance test

For the GTT, after an overnight fast, the mice were injected intraperitoneally with glucose (2 g/kg body weight). For the ITT, 6-h fasted mice were given an intraperitoneal injection of insulin (1 unit/kg body weight). Blood glucose concentrations were determined with a One-Touch Ultra® glucometer (LifeScan Inc., Milpitas, CA) at 0, 15, 30, 60, 90, and 120 min after injection.

Flow cytometric analysis

SVF cells were isolated from epididymal white adipose tissue and stained with phycoerythrin-conjugated anti-mouse F4/80 antibody and FITC-conjugated anti-mouse CD11b antibody. The cells were analyzed on a CytoFlex (Beckman, CA) with CellQuest software (BD Biosciences).

Histology and immunostaining

To detect RORα protein expression in RAW 264.7 cells, the cells were mounted on chrome alum–coated slides. The slides were fixed with 3.7% (v/v) formaldehyde in PBS (pH 7.4) and then blocked in PBS with 6% normal donkey serum and 0.3% Triton X-100. Thereafter, the cells were incubated with a rabbit anti-mouse RORα antibody (1:100 dilution). After washing in PBS-Tween 0.02%, the cells were immunostained with Alexa Fluor-conjugated goat anti-rabbit antibodies (1:500; Life Technologies). The nuclei were counterstained with DAPI (Life Technologies).

To examine the macrophage infiltration into the adipose tissue, isolated adipose tissue was fixed overnight in 10% neutral buffered formalin. Samples were then dehydrated with ethanol, embedded in paraffin, and sectioned (4 μm). Sections of adipose tissue were stained with a rabbit anti-mouse F4/80 antibody and an avidin-biotin-peroxidase detection system.

The slides were mounted with Entellan. Image analysis was performed with a fluorescence upright microscope (Zeiss Axio Imager). F4/80-positive cells in at least six randomly selected fields in sections from five different mice were counted.

Quantitative real-time PCR analysis

Total RNA was extracted from RAW264.7 cells, 3T3-L1 adipocytes, or epididymal adipose tissue of ob/ob mice using TRIzol reagent. RNA concentrations were measured with the NanoDrop ND-100 spectrophotometer (NanoDrop Technologies, Wilmington, DE). cDNA synthesis and quantitative real-time PCR analysis were performed as described (35). Briefly, the cDNA samples were mixed with SYBR Green Master Mix and gene-specific primers (Table 1) in a total volume of 25 μl. PCR was performed in 96-well optical reaction plates with an ABI PRISM 7500 sequence detection system (Applied Biosystems). Cycling parameters were 2 min at 50 °C, 10 min at 95 °C, and 40 cycles of 15 s at 95 °C and 1 min at 60 °C. The results were normalized to the expression of GAPDH, and a comparative *Ct* ($\Delta\Delta Ct$) was applied to the raw *Ct* values to establish the relative gene expression between groups. PCR was done in triplicate.

Protein extraction and Western blotting

Protein extraction and Western blotting were performed as described previously (21). In brief, epididymal adipose tissue or adipocytes were lysed in radioimmune precipitation assay buffer. Protein concentration was measured using a BCA protein assay kit; 20 μg proteins from each sample was separated by 10% SDS-PAGE, then transferred to a polyvinylidene difluoride membrane, and immunoblotted with the indicated primary antibodies. The blots were then washed and subsequently incubated with the secondary horseradish peroxidase–conjugated antibodies. Signals were visualized by using an enhanced chemiluminescence kit according to the manufacturer's instructions and quantified using UN-SCAN-IT Gel 5.1 software (Silk Scientific Inc., Orem, UT).

Statistical analysis

All of the data were shown as means ± S.D. with at least three independent experiments. Statistical analysis was performed using GraphPad Prism and Student's *t* test. $p < 0.05$ was considered statistically significant.

Author contributions—Y. L., Y. C., and J. Z. performed all the experiments with help from Y. L., and Y. Z. and Z. S. analyzed the data. Y. L and Z. S. drafted the manuscript. Z. S. supervised the project. All authors reviewed the results and approved the final version of the manuscript.

References

1. Weisberg, S. P., McCann, D., Desai, M., Rosenbaum, M., Leibel, R. L., and Ferrante, A. W., Jr. (2003) Obesity is associated with macrophage accumulation in adipose tissue. *J. Clin. Invest.* **112,** 1796–1808
2. Wellen, K. E., and Hotamisligil, G. S. (2003) Obesity-induced inflammatory changes in adipose tissue. *J. Clin. Invest.* **112,** 1785–1788
3. Wensveen, F. M., Valentić, S., Sestan, M., Turk Wensveen, T., and Polić, B. (2015) The "Big Bang" in obese fat: events initiating obesity-induced adipose tissue inflammation. *Eur. J. Immunol.* **45,** 2446–2456
4. Saltiel, A. R., and Olefsky, J. M. (2017) Inflammatory mechanisms linking obesity and metabolic disease. *J. Clin. Invest.* **127,** 1–4
5. Giguère, V., Tini, M., Flock, G., Ong, E., Evans, R. M., and Otulakowski, G. (1994) Isoform-specific amino-terminal domains dictate DNA-binding properties of ROR α, a novel family of orphan hormone nuclear receptors. *Genes Dev.* **8,** 538–553
6. Solt, L. A., and Burris, T. P. (2012) Action of RORs and their ligands in (patho)physiology. *Trends Endocrinol. Metab.* **23,** 619–627
7. Jetten, A. M., Kang, H. S., and Takeda, Y. (2013) Retinoic acid-related orphan receptors α and γ: key regulators of lipid/glucose metabolism, inflammation, and insulin sensitivity. *Front. Endocrinol.* (*Lausanne*) **4,** 1
8. Gold, D. A., Gent, P. M., and Hamilton, B. A. (2007) RORα in genetic control of cerebellum development: 50 staggering years. *Brain Res.* **1140,** 19–25
9. Stapleton, C. M., Jaradat, M., Dixon, D., Kang, H. S., Kim, S. C., Liao, G., Carey, M. A., Cristiano, J., Moorman, M. P., and Jetten, A. M. (2005) Enhanced susceptibility of staggerer (RORα sg/sg) mice to lipopolysaccharide-induced lung inflammation. *Am. J. Physiol. Lung Cell Mol. Physiol.* **289,** L144–L152
10. Delerive, P., Monté, D., Dubois, G., Trottein, F., Fruchart-Najib, J., Mariani, J., Fruchart, J. C., and Staels, B. (2001) The orphan nuclear receptor ROR α is a negative regulator of the inflammatory response. *EMBO Rep.* **2,** 42–48
11. Jaradat, M., Stapleton, C., Tilley, S. L., Dixon, D., Erikson, C. J., McCaskill, J. G., Kang, H. S., Angers, M., Liao, G., Collins, J., Grissom, S., and Jetten, A. M. (2006) Modulatory role for retinoid-related orphan receptor α in allergen-induced lung inflammation. *Am. J. Respir. Crit. Care Med.* **174,** 1299–1309
12. Kang, H. S., Okamoto, K., Takeda, Y., Beak, J. Y., Gerrish, K., Bortner, C. D., DeGraff, L. M., Wada, T., Xie, W., and Jetten, A. M. (2011) Transcriptional profiling reveals a role for RORα in regulating gene expression in obesity-associated inflammation and hepatic steatosis. *Physiol. Genomics* **43,** 818–828
13. Hotamisligil, G. S., and Davis, R. J. (2016) Cell signaling and stress responses. *Cold Spring Harb. Perspect. Biol.* **8,** a006072
14. Walter, P., and Ron, D. (2011) The unfolded protein response: from stress pathway to homeostatic regulation. *Science* **334,** 1081–1086
15. Ozcan, U., Cao, Q., Yilmaz, E., Lee, A. H., Iwakoshi, N. N., Ozdelen, E., Tuncman, G., Görgün, C., Glimcher, L. H., and Hotamisligil, G. S. (2004) Endoplasmic reticulum stress links obesity, insulin action, and type 2 diabetes. *Science* **306,** 457–461
16. Kawasaki, N., Asada, R., Saito, A., Kanemoto, S., and Imaizumi, K. (2012) Obesity-induced endoplasmic reticulum stress causes chronic inflammation in adipose tissue. *Sci. Rep.* **2,** 799
17. Ghosh, A. K., Garg, S. K., Mau, T., O'Brien, M., Liu, J., and Yung, R. (2015) Elevated endoplasmic reticulum stress response contributes to adipose tissue inflammation in aging. *J. Gerontol. A. Biol. Sci. Med. Sci.* **70,** 1320–1329
18. Pagliassotti, M. J., Kim, P. Y., Estrada, A. L., Stewart, C. M., and Gentile, C. L. (2016) Endoplasmic reticulum stress in obesity and obesity-related disorders: an expanded view. *Metabolism* **65,** 1238–1246
19. Lee, J., and Ozcan, U. (2014) Unfolded protein response signaling and metabolic diseases. *J. Biol. Chem.* **289,** 1203–1211
20. Wang, Y., Kumar, N., Nuhant, P., Cameron, M. D., Istrate, M. A., Roush, W. R., Griffin, P. R., and Burris, T. P. (2010) Identification of SR1078, a synthetic agonist for the orphan nuclear receptors RORα and RORγ. *ACS Chem. Biol.* **5,** 1029–1034
21. Kuang, J., Hou, X., Zhang, J., Chen, Y., and Su, Z. (2014) Identification of insulin as a novel retinoic acid receptor-related orphan receptor α target gene. *FEBS Lett.* **588,** 1071–1079
22. Liu, Y., Zhang, Y., Zhang, J., Feng, P., and Su, Z. (2017) Obesity-induced endoplasmic reticulum stress suppresses nuclear factor-Y expression. *Mol. Cell Biochem.* **426,** 47–54
23. Hotamisligil, G. S. (2010) Endoplasmic reticulum stress and the inflammatory basis of metabolic disease. *Cell* **140,** 900–917
24. Lu, P. D., Harding, H. P., and Ron, D. (2004) Translation reinitiation at alternative open reading frames regulates gene expression in an integrated stress response. *J. Cell Biol.* **167,** 27–33

25. Solt, L. A., Kumar, N., Nuhant, P., Wang, Y., Lauer, J. L., Liu, J., Istrate, M. A., Kamenecka, T. M., Roush, W. R., Vidović, D., Schürer, S. C., Xu, J., Wagoner, G., Drew, P. D., Griffin, P. R., *et al.* (2011) Suppression of TH17 differentiation and autoimmunity by a synthetic ROR ligand. *Nature* **472,** 491–494
26. Jiang, H. Y., Wek, S. A., McGrath, B. C., Scheuner, D., Kaufman, R. J., Cavener, D. R., and Wek, R. C. (2003) Phosphorylation of the α subunit of eukaryotic initiation factor 2 is required for activation of NF-κB in response to diverse cellular stresses. *Mol. Cell Biol.* **23,** 5651–5663
27. Urano, F., Wang, X., Bertolotti, A., Zhang, Y., Chung, P., Harding, H. P., and Ron, D. (2000) Coupling of stress in the ER to activation of JNK protein kinases by transmembrane protein kinase IRE1. *Science* **287,** 664–666
28. Seki, E., Brenner, D. A., and Karin, M. (2012) A liver full of JNK: signaling in regulation of cell function and disease pathogenesis, and clinical approaches. *Gastroenterology* **143,** 307–320
29. Wang, S., Dougherty, E. J., and Danner, R. L. (2016) PPARγ signaling and emerging opportunities for improved therapeutics. *Pharmacol. Res.* **111,** 76–85
30. Zenri, F., Hiroi, H., Momoeda, M., Tsutsumi, R., Hosokawa, Y., Koizumi, M., Nakae, H., Osuga, Y., Yano, T., and Taketani, Y. (2012) Expression of retinoic acid-related orphan receptor α and its responsive genes in human endometrium regulated by cholesterol sulfate. *J. Steroid Biochem. Mol. Biol.* **128,** 21–28
31. Nakagawa, T., Zhu, H., Morishima, N., Li, E., Xu, J., Yankner, B. A., and Yuan, J. (2000) Caspase-12 mediates endoplasmic-reticulum-specific apoptosis and cytotoxicity by amyloid-β. *Nature* **403,** 98–103
32. Murakami, T., Saito, A., Hino, S., Kondo, S., Kanemoto, S., Chihara, K., Sekiya, H., Tsumagari, K., Ochiai, K., Yoshinaga, K., Saitoh, M., Nishimura, R., Yoneda, T., Kou, I., Furuichi, T., *et al.* (2009) Signalling mediated by the endoplasmic reticulum stress transducer OASIS is involved in bone formation. *Nat. Cell Biol.* **11,** 1205–1211
33. Hetz, C. (2012) The unfolded protein response: controlling cell fate decisions under ER stress and beyond. *Nat. Rev. Mol. Cell Biol.* **13,** 89–102
34. Lu, M., and Varley, A. W. (2013) Harvest and culture of mouse peritoneal macrophages. *Bio-protocol.* **3,** e976
35. Su, Z., Leduc, M. S., Korstanje, R., and Paigen, B. (2010) Untangling HDL quantitative trait loci on mouse chromosome 5 and identifying Scarb1 and Acads as the underlying genes. *J. Lipid Res.* **51,** 2706–2713